Electrodeposition of Co + Ni alloys on modified silicon substrates

E. GÓMEZ and E. VALLÉS
Laboratori de Ciència i Tecnologia Electroquímica de Materials, Departament de Química física, Universitat de Barcelona, Martí i Franquès 1, 08028 Barcelona, Spain
(correspondence, e-mail: e.gomez@qf.ub.es; e.valles@qf.ub.es; fax: +34 93 4021231)

Abstract

Cobalt + nickel alloys were electrodeposited on different base-silicon substrates since these alloys are interesting for several magnetic device applications. Acid chloride baths were used to obtain magnetic cobalt + nickel layers directly over silicon surfaces, tantalum silicide or metallic seed-layers. Although the initial stages of nucleation were influenced by the kind of substrate, in all substrates nucleation and three-dimensional growth evolving to compact, fine-grained and homogeneous deposition, took place. Preferential deposition of cobalt and anomalous codeposition occurred. Different compositions of the alloy were obtained, as is normal with a solid–solution formation. The cobalt content in the deposit rose with increase in both cobalt(II) and saccharin concentrations and fell with decrease in the applied potential or current density.

1. Introduction

Magnetic alloys have been at the centre of attention of both experimental researchers and theoreticians over the last few years, due to their importance to the electronics industries. Numerous studies have been devoted to the analysis of magnetic alloys produced by electroplating. Ferromagnetic alloys have received considerable attention due to their extensive applications in microelectronics and magnetic media [1–7]. The electroplating of Co + Ni alloys have been studied because of their various magnetic device applications, especially in microsystems technology used to manufacture sensors and actuators. The manufacture of devices such as microrelays and inductors has also used magnetic materials as driving members [8, 9].

The Co + Ni system has the advantage that its magnetic characteristics shift from soft magnetic for low cobalt content to permanent magnetic for higher cobalt containing alloys [10]. Moreover, the Co + Ni alloy forms a solid solution over the whole concentration range, which enables the alloy to be obtained with any proportion of the two metals. In a preliminary study the authors reported codeposition of nickel and cobalt on vitreous carbon substrate from a chloride bath at low total metal concentration [11]. The study, centred on the first stages of the deposition process, mapped the sequence of steps by means of which the alloy deposition took place.

The electrodeposition of Co + Ni belongs to the anomalous type [12], in which the less noble metal (cobalt) is preferentially deposited. This is expressed by the fact that the percentage of cobalt in the deposit is much higher than the percentage of cobalt in the bath. Taking into account anomalous codeposition, the bath composition proposals were always solutions in which there was more nickel.

There is little literature on the electrochemical alloy deposition on semiconductor substrates. Due to the interest in the direct application of Co + Ni films on this kind of substrate, the objectives of this study were as follows: (i) to determine whether the general electrochemical behaviour observed on a metallic substrate also applies on semiconductors and to characterize the alloy deposition under these conditions and (ii) to establish the relationship between the deposition parameters and both the deposit composition and morphology. The total metal concentration value was increased compared to that used in the previous study, in order to increase the deposition rate, since it seemed

likely that, on these modified silicon substrates, the deposition process would be slow.

The deposits were obtained from simple solutions containing boric acid and chloride salts of both metals in the hope that the low complexity of this bath would allow easy chemical control. During the deposition of thin layers by electrochemical methods, internal stress almost always develops [13–16]. In order to minimize the internal stresses of the Co + Ni electrodeposits, saccharin was added to the bath.

2. Experimental details

The electrolyte solutions always contained excess of Ni(II) and were freshly prepared from $NiCl_2.6H_2O$, $CoCl_2.6H_2O$, H_3BO_3 and saccharin. All reagents were analytical grade from Merck. The [Ni(II)] varied between 0.7 and 1 mol dm^{-3} and [Co(II)] between 0.1 and 0.4 mol dm^{-3}, but the total metal concentration was always 1.1 mol dm^{-3}. The boric acid content was 30 g dm^{-3} and the saccharin content varied between 0.5 and 0.9 g dm^{-3}. The solution pH was adjusted to 3 for all experiments to minimize the hydrogen evolution and the possible precipitation of hydroxylated species. Water was distilled twice and then treated with a Milipore Milli Q system.

Substrates used in this study were monocrystalline (1 0 0) silicon wafers (p/n^+ or p/p^+-type) and tantalum silicide with and without silicon oxide masks. To improve the adhesion of deposits silicon with sacrificial titanium and nickel seed layers obtained by sputtering were also used. For p/n^+ and p/p^+ silicon samples, the native oxide layer was etched in an aqueous HF solution (10%) for a few seconds, until the sample exhibited hydrophobic behaviour. Tantalum silicide samples were etched in HF solution to improve the adhesion of the final deposit. Samples of silicon with sacrificial seed layers were degreased in a strong basic solution for two minutes and rinsed with water until they had a mirror appearance. In all cases, the samples were inmersed in the solution inmediately.

The reference electrode was Ag/AgCl connected to the cell via in a Luggin capillary containing 1 mol dm^{-3} NaCl solution. All potentials are referred to this electrode. A nickel sheet was used as counterelectrode. Solutions were deaerated with argon and the temperature was maintained constant in the 20 and 60 °C range.

Electrochemical experiments were carried out in a conventional three-electrode cell using an EG&G 273 model potentiostat/galvanostat controlled by a micro-computer. The morphology of deposits was examined with a Hitachi S 2300 or a Leica Cambridge Stereoscan

S-360 scanning electron microscopes. Electrodeposits were analysed using the X-ray analyser incorporated either in a Cambridge L-120 scanning electron microscope or in an electron microprobe Cameca SX-50. The magnetic measurements were performed with a Manics DSM 8 pendulum-type magnetometer at room temperature.

3. Results

A general study of cobalt + nickel electrodeposition, centred on the initial stages of the process, was performed for several base-silicon substrates, using different electrochemical techniques.

3.1. Modified silicon substrates

The possibility of depositing directly on doped silicon surfaces was investigated using voltammetry. Figure 1 shows a voltammogram at 50 mV s^{-1} obtained on silicon p/n^+ substrate for a $NiCl_2$ 0.9 mol dm^{-3} + $CoCl_2$ 0.2 mol dm^{-3} + saccharin 0.7 g dm^{-3} at pH 3 solution. When the scan was reversed at the onset of the voltammetric current, negative current was obtained during the positive going sweep. Oxidation current began to appear around −400 mV and only a non-symmetrical peak, whose maximun was slightly dependent on the cathodic potential limit, was obtained.

For the potentiostatic experiments a monotonic current increase was observed in the current-time transients followed by a quasi-stabilization of the current (Figure 2). In the potential range studied, no diminution in current value was observed on the curve feature. In any case the stirring of the solution did not affect the current value registered.

Figure 3 shows the potential–time dependence for the deposition of cobalt-nickel alloy on silicon substrate at
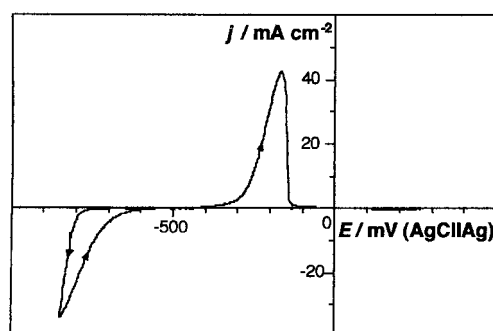

Fig. 1. Cyclic voltammogram of a 0.9 mol dm^{-3} $NiCl_2$ + 0.2 mol dm^{-3} $CoCl_2$ + 0.7 g dm^{-3} saccharin solution. pH 3. $T = 50$ °C. p/n^+ silicon substrate. $v = 50$ mV s^{-1}.
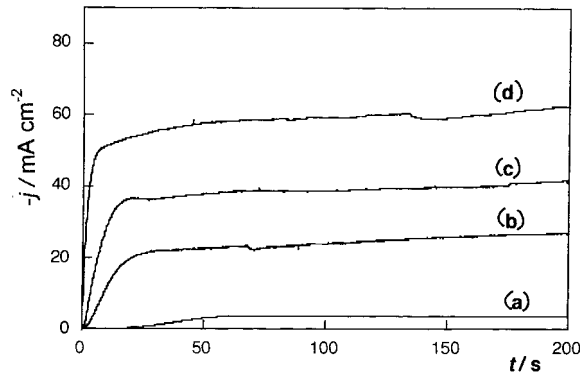
Fig. 2. j/t transients at (a) -700, (b) -750, (c) -800 and (d) -850 mV. Same solution, temperature and substrate that in Figure 1.
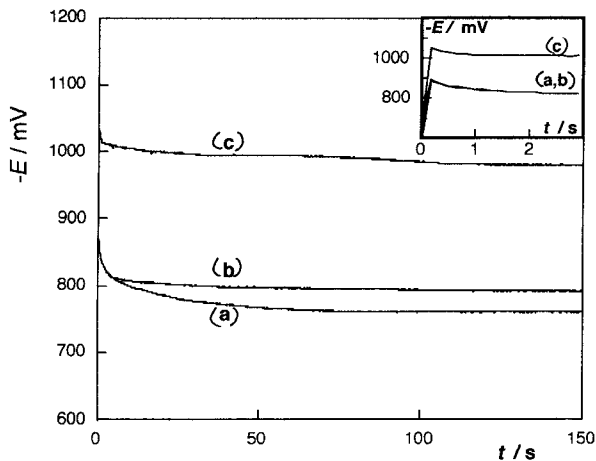

Fig. 3. E/t transients at (a) -24, (b) -35 and (c) -127 mA cm^{-2}. Same solution, temperature and substrate that in Figure 1.

Fig. 4. Cyclic voltammogram of the same conditions that in Figure 1, but over p/p$^+$ silicon substrate.

that the previously obtained on p/n$^+$ silicon substrate at 50 °C.

The morphological study of the deposits showed that their morphology was not dependent on the technique used (potentiostatic/galvanostatic) to obtain the alloy. Moreover, for all substrates, where the deposition was made on samples provided with masks of silicon oxide, it was observed that the deposition was selective and did not occur on silicon oxide (Figure 5). Polyhedral crystallites were obtained at low potentials/current densities, short deposition times and in nonstirred conditions (Figure 6(a)). The grain size was gradually refined on decreasing the potential/current density. However, for the more negative values, some acicular crystallites were also observed (Figure 6(b)). This directional growth was minimized by stirring the solution during the electrodeposition.

These experimental results indicate that the bath tested enables Co + Ni to be deposited directly over several modified silicon surfaces. However, the deposits

different current densities (Figure 3). The potential–time transients present a potential spike with a gradual decrease to a steady value. Both spike and steady potential values were more negative as the current density was made more negative. The spike potential is related with the high overpotential necessary to begin the deposition process. When this potential had been achieved, nucleation began and deposition continued at a steady value depending on the current applied: more negative as the current density increased.

The cobalt–nickel deposition was also possible on other modified silicon substrates, but the deposition rate was markedly different depending the kind of substrate. When p/p$^+$ silicon was used, a slow deposition process took place, as indicated by the smaller current–potential slope in the voltammetric curve (Figure 4) than that observed for p/n$^+$ substrates at the same temperature. In contrast, when tantalum silicide was used, room temperature was sufficient to attain similar deposition rates
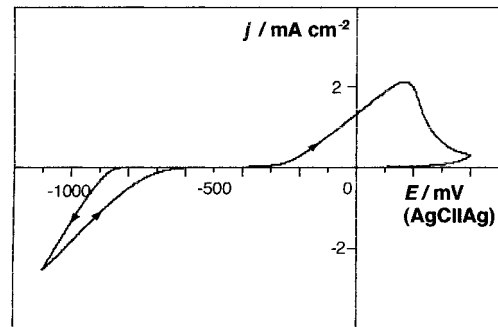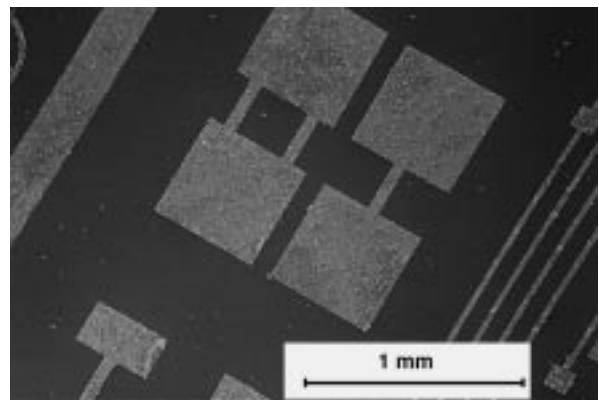

Fig. 5. SEM images of deposits obtained on Si/SiO$_2$/tantalum silicide with SiO$_2$ mask dispositives from a 0.8 mol dm^{-3} NiCl$_2$ + 0.3 mol dm^{-3} CoCl$_2$ + 0.5 g dm^{-3} saccharin solution. pH 3. $T = 25$ °C. 25 min at -850 mV.
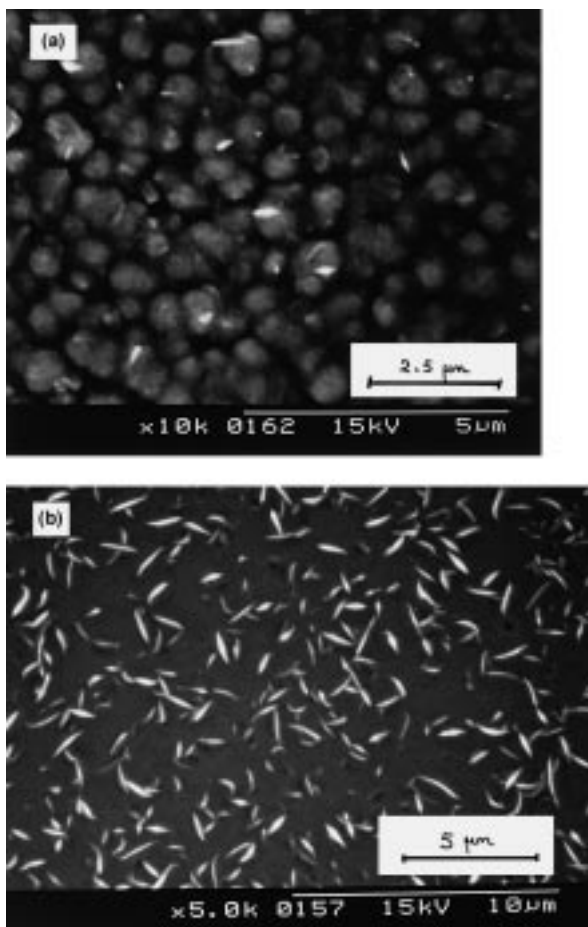
Fig. 6. SEM images of deposits obtained at (a) -24 mA cm^{-2} during 200 s, (b) -130 mA cm^{-2} during 200 s. Same solution, temperature and substrate that in Figure 1.

in this case are not adherent and would not be useful for many applications.

3.2. *Nickel–titanium seed layer*

The influence of bath composition and deposition technique on the composition and morphology of deposits was studied using seed layers. The metallic seed-layer was used to increase the adhesion of the electrodeposited alloy to the substrate. A titanium–nickel film was chosen because good adhesion is expected between titanium and the silicon substrate, and between nickel and the alloy coating.

The electrochemical study of Co + Ni deposition on the seed-layer showed a similar behaviour to that observed previously on modified silicon substrates. Although the alloy could be electrodeposited at room temperature on this substrate, since high temperatures typically favour the formation of less stressed layers,
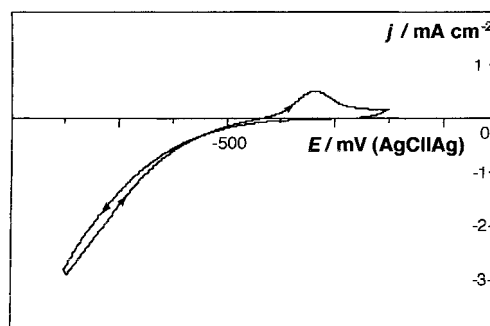

Fig. 7. Cyclic voltammogram of the same solution and temperature that in Figure 1, but over Si/SiO$_2$/Ti/Ni substrate.

50 °C was selected. In these conditions, less negative potentials were necessary to begin the alloy electrodeposition. In voltammetric experiments (Figure 7) the peak, corresponding to the oxidation of the alloy was also slightly moved to more positive potentials when the cathodic limit was made gradually more negative, so that, in some conditions, the oxidation peak of the alloy overlapped with the oxidation current of the seed layer.

Over the Ti–Ni seed layer, potentiostatic and galvanostatic electrodeposition conditions lead to deposits that, after a longer deposition time, remained linked to the substrate even when their thickness attained several microns. This result allowed study of the characteristics of the Co + Ni alloy coating by modifying the electrodeposition conditions.

The alloy deposits were obtained using both potentiostatic and galvanostatic techniques. In the potentiostatic experiments the applied potential range was selected between -700 and -900 mV in order to counterbalance the deposition rate value and the minimization of hydrogen evolution. In galvanostatic experiments the current density applied was adjusted so that the value of the steady state potential attained during the experiment was in the potentiostatic range. In all cases the solution was stirred moderately (using argon flow) throughout the deposition to maintain homogeneous deposit composition.

For all bath compositions studied, the analysis of the deposits, even those obtained for very low deposition times at either low overpotentials/current densities, revealed that the coatings were always homogeneous, compact, and fine-grained (Figure 8); their structure was difficult to observe. On these substrates, because of the high nuclei density, coalescence occurred at very low deposition times, so that individual grains could not be resolved.

The deposits obtained at fixed electrodeposition conditions and for variable deposition times show the same composition (Table 1). These results together with the
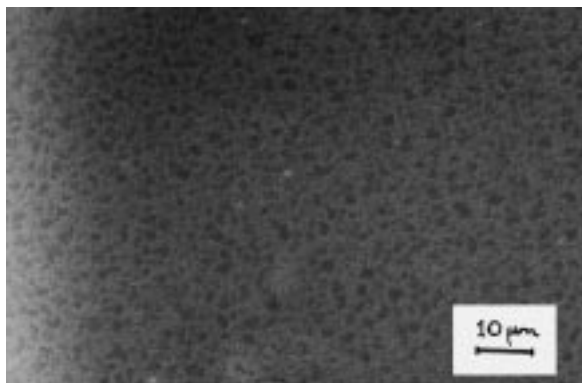
Fig. 8. SEM image of the deposit obtained at stirring conditions at -24 mA cm^{-2} during 90 min. Same solution, temperature and substrate that in Figure 7.

results of the ESCA experiments (Figure 9) confirmed that, in stirred conditions, a constant alloy composition throughout the thickness of the deposit was assured.

For a fixed bath, the composition of the alloy was similar with potentiostatic or galvanostatic techniques (Table 1). As occurred with a vitreous carbon substrate [11], the percentage of cobalt in the deposit was higher than in the solution and the deposits were always cobalt-rich, as expected in anomalous codeposition, although the cobalt content in the deposit decreased when the potential/current density applied was made more negative.

When different baths were tested the results showed that the composition of the alloy was highly dependent on the concentration of the metallic cations in the solution (Table 2). For example, when the concentration of cobalt(II) in the solution was 0.3 mol dm^{-3}, the deposit was very rich in cobalt. If this concentration increased, the deposit was quasi-pure cobalt. And on increasing the saccharin concentration, the Co/Ni ratio in the deposit was enhanced.

The rate of growth was determined by measuring the thickness of the coating at different deposition times.

Table 1. Influence of the applied potential in potentiostatic conditions or the current density in galvanostatic conditions on the Co/Ni ratio on the deposits
Bath composition: 0.9 mol dm^{-3} Ni(II) + 0.2 mol dm^{-3} Co(II) + 0.7 g dm^{-3} saccharin. Si/SiO$_2$/Ti/Ni substrate. **Est** is the stationary potential in the galvanostatic deposition

Potentiostatic deposition			Galvanostatic deposition			
E/mV	t/min	Co/Ni	j/mA cm^{-2}	t/min	**Est**/mV	Co/Ni
-750	90	2.5	-7.5	90	-730	2.4
-800	30	2.2	-9.5	90	-750	2.2
-800	90	2.2	-11.5	90	-800	2.2
-850	90	2.1	-30.9	90	-830	1.8

The results indicate that an increase in the overpotential favours the growth rate (Table 2). However, very negative values of applied potential were not adequate because under these conditions the electrodeposition process is less efficient as a consequence of simultaneous hydrogen evolution.

Since the applications of the alloy films are dependent on their soft or permanent magnetic behaviour, the magnetic properties of some coatings were tested via hysteresis loops. Controlling the deposition conditions enabled films with different coercitivity (H_c) values to be obtained, although the saturation magnetization (M_s) value was very similar for all conditions (Figure 10). Logically, coercitivity is enhanced when the cobalt content in the coating increased. However, the H_c value must also be dependent on the morphology and structure of the film.

4. Discussion

These results show that the chloride bath tested permits cobalt + nickel magnetic layers of different compositions to be electrodeposited over several silicon-based surfaces at moderate temperatures. Moreover, control of the electrodeposition conditions leads to films which can be used for different magnetic applications.

From the electrochemical experiments it was deduced that alloy deposition behaves similarly on different surfaces. The general trends of Co + Ni alloy deposition are similar, although the overpotential at the start of the crystallization is obviously influenced by the substrate. The voltammetric current loop, the monotonic rises in the potentiostatic transients and the nucleation potential spike observed in the galvanostatic experiments indicate [17–19] that the cobalt–nickel deposition begins by a process of nucleation and growth, as occurs on other substrates [11, 20].

The voltammetric study of the cobalt + nickel alloy depositon on different substrates shows the inclusion of the entire alloy oxidation charge in only one peak, as occurs for the oxidation of other solid solutions [20, 21]. The fact that the oxidation potentials of nickel and pure cobalt are close [22, 23], and that the structure of a cobalt + nickel alloy is similar to that of the separate metals might explain why the oxidation occurs in a single peak. However, the maximum of the oxidation peak depends on the cathodic limit as a consequence of the variation of alloy composition, which is consistent with the results obtained for more dilute baths [11] .

The chloride bath used is simple, since it needs only one buffering agent and one additive to provide homo-
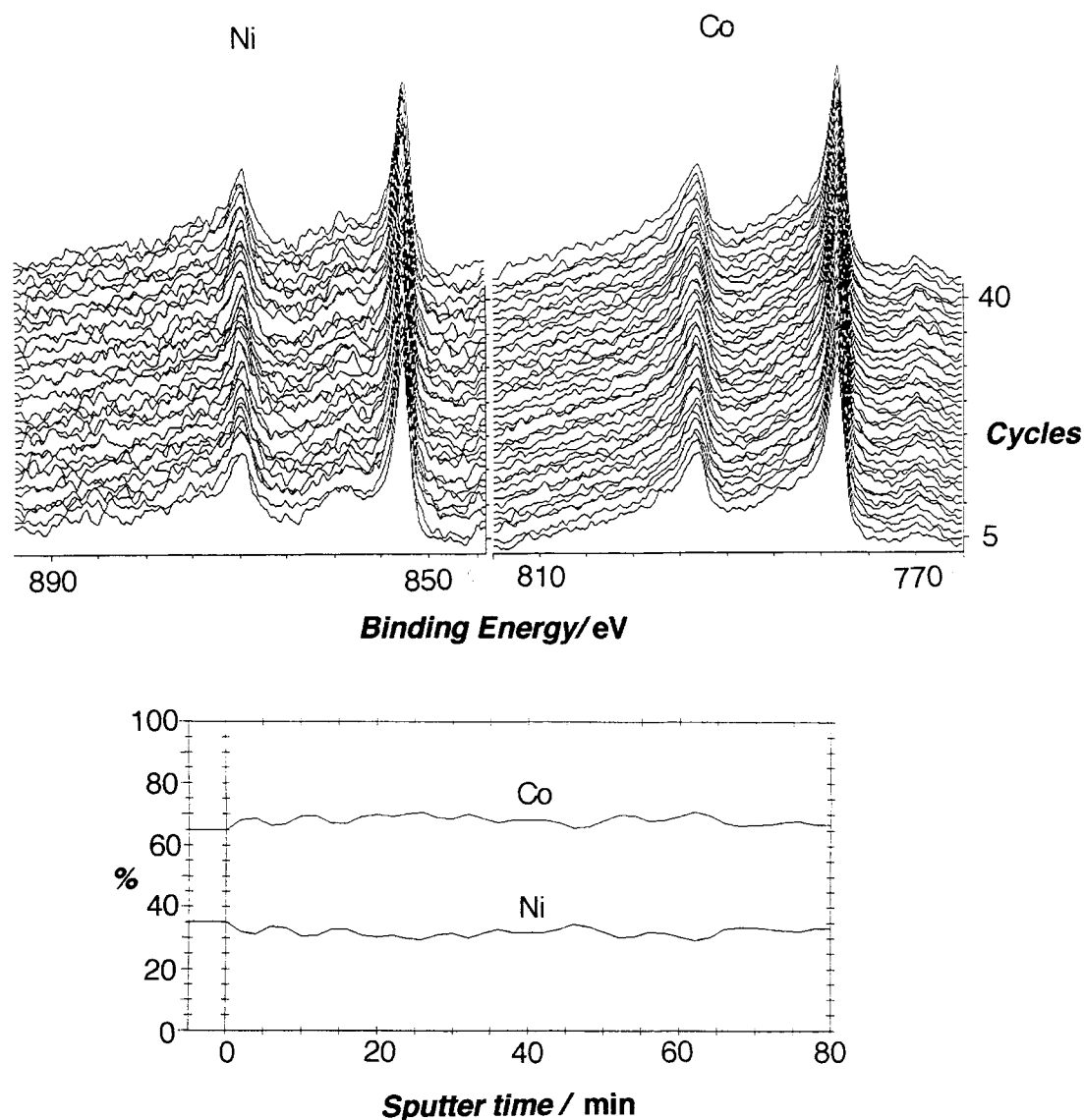
Fig. 9. ESCA depth profiles of a deposit obtained at −800 mV during 30 min. Same solution, temperature and substrate that in Figure 7.

Table 2. Influence of bath composition on the Co/Ni ratio on the deposits at different applied potentials. Si/SiO$_2$/Ti/Ni substrate

[Ni(II)]	[Co(II)]	[sac]/g dm^{-3}	E/mV	t/min	Co/Ni	V_{dep}/μm h^{-1}
0.9	0.2	0.5	−750	90	1.6	
			−800	90	1.5	
			−850	90	1.4	
0.8	0.3	0.5	−750	90	7.0	
			−800	90	4.7	
			−850	90	4.1	
		0.9	−700	90	8.3	
			−700	225	8.2	2.9
			−775	90	7.4	5.7
			−800	90	6.9	
			−850	90	5.9	11.3

geneous fine-grained films. The control of the bath is, therefore, easy.

The results indicate that by combining composition and plating conditions, it is possible to deposit alloy directly on silicon substrates after removal of the native oxides. Moreover, the deposition is selective and does not occur on silicon oxide, which permits the manufacture of microstructures. However, due to the low deposit adhesion, for this kind of surface the method is only appropriate when the surface is to be modified by nano- or micro-alloy particles or when very thin magnetic films are needed. When films several microns thick are required, it is best to use intermediate seed-layers, since they improve adhesion to the substrate.
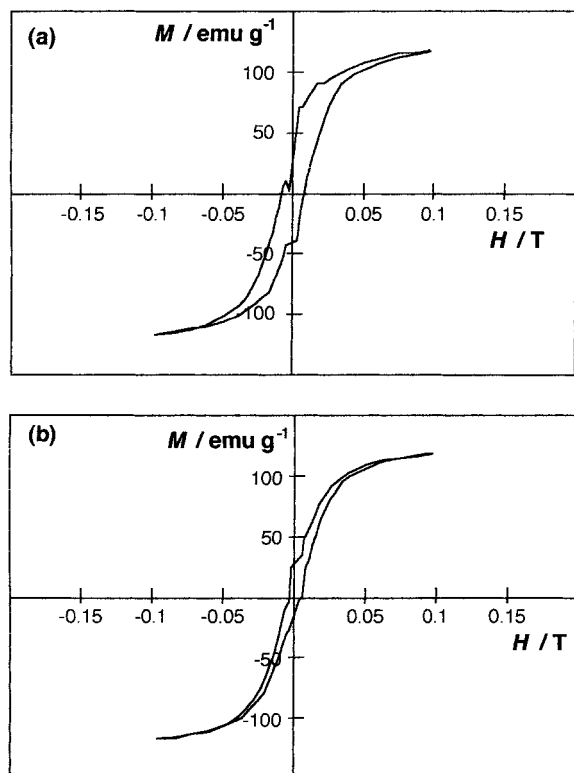
Fig. 10. Magnetic hysteresis curves of a deposit obtained on Si/SiO$_2$/Ti/Ni substrate. 90 min at -800 mV. $T = 50\,^{\circ}$C. (a) 0.8 mol dm^{-3} NiCl$_2$ + 0.3 mol dm^{-3} CoCl$_2$ + 0.9 g dm^{-3} saccharin solution. Alloy composition: 13% Ni + 87% Co. (b) 0.9 mol dm^{-3} NiCl$_2$ + 0.2 mol dm^{-3} CoCl$_2$ + 0.7 g dm^{-3} saccharin solution. Alloy composition: 32% Ni + 68% Co.

The nature of the substrate affects the size of the initial crystallites: when the deposit was initially formed on seed-layer substrates, there was more nucleation and a larger number of small nuclei than when the deposition took place directly on a silicon substrate. However, irrespective of the kind of surface, the final deposits obtained in parallel conditions are always similar because the effect of the substrate is not relevant at high deposition times, since the growth modes are similar.

The cobalt + nickel deposition always leads to a solid solution, which allows coatings with different composition to be obtained in such away that the metal percentage in the coating can be varied continuously. Different alloy compositions can be obtained by modifying the electrodeposition parameters, although cobalt is preferentially electrodeposited, as expected for an anomalous codeposition. Thus, for a fixed bath composition, the alloy composition can be adjusted via the potential/current density applied or by varying the saccharin concentration. The cobalt content increases with both cobalt(II) and additive concentration, whereas it decreases with the decrease of the applied potential.

High concentrations of electroactive cations and gentle stirring of the solution prevent the depletion of cobalt(II), which is the less concentrated electroactive species, in the environment of the electrode during the deposition process. A moderate pH (pH 3) and stirring of the solution also prevent variation in the local pH, caused by simultaneous hydrogen evolution, which can lead to precipitation of hydroxides.

The deposit growth rate increased as the applied potential was made more negative, but high negative potential/current values are not suitable because hydrogen evolution must be avoided. However, in all cases, the rate of growth of the deposit is not very high, probably due to the adsorption of species present in the bath. High metal concentrations are useful in order to avoid low deposition rates.

Anomalous codeposition on all the substrates analysed occurs in a similar way to that observed in a simple chloride bath on vitreous carbon substrate [11]. A mechanism for anomalous cobalt + nickel deposition was proposed, in which the adsorption of Co(II) species over the first electrodeposited nickel was responsible for the inhibition for the subsequent nickel deposition. In the bath studied, the presence of boric acid and saccharin may influence the deposition mechanism, although the possible adsorption of these species does not avoid the preferential cobalt deposition.

The experimental data show that this chloride bath is suitable for plating alloys of nickel with cobalt. These results will be used as a starting point for the development of conditions which allow adequate coatings in all applications.

Acknowledgements

References

1. L.T. Romankiw, *Electrochim. Acta* **42** (1997) 2985.
2. W. Stark and W. Bacher, *Galvanotechnik* **83** (1993) 2946.

3. D.E. Spelotis, G. Bate, J.K. Alstad and J.R. Morrison, *J. Appl. Phys.* **36** (1965) 972.

4. B. Lochel, A. Maciossek, H. Quenzer and B. Wagner, *J. Electrochem. Soc.* **143** (1996) 237.

5. B. Lochel and A. Maciossek, *J. Electrochem. Soc.* **143** (1996) 3343.

6. W.P. Taylor, M. Schneider, H. Baltes and M.G. Allen, Transducers **97**. International conference on *Solid State Sensors and Actuators*, Chicago (1997) p. 1445

7. G. Bate, In: E.P. Wohlfarth, (ed.) *Ferromagnetic Materials*, vol. 2, North Holland, 1980 chapter 7, p. 381.

8. B. Lochel, A. Maciossek, H. Quenzer and B. Wagner, *Sensors & Actuators A* **46** (1995) 98.

9. W. Tang, V. Temesvary, Yu-C.Tai and D.K. Miu, In: L.T. Romankiw and D.A. Herman (eds), *Magnetic Materials, Processes and Devices*, **PV95**-18, The Electrochemical Society Proceedings Series Pennington, (1996) NJ, p. 461.

10. P.C. Andricacos, In: M. Paunovic (ed.) *Electrochemically Deposited Thin Films II*, **PV94**-31, The Electrochemical Society Proceedings Series Pennington, (1995) NJ, p. 157.

11. E. Gómez, J. Ramirez and E. Vallés, *J. Appl. Electrochem.* **28** (1998) 71.

12. A. Brenner, *Electrodeposition of Alloys*, vol. 2, Academic Press, New York 1963.

13. S. Armyanov, *Metal Finish.* **91** (1993) 42.

14. G. Sotirova-Chakarova and S. Armyanov, *J. Electrochem. Soc.* **137** (1990) 3551.

15. T.R. Mc Guire and T.S. Plaskett, *J. Appl. Phys.* **75** (1994) 6537.

16. T.A. Tochitski, A.V. Boltushin and V.G. Shadrov, *Russ. J. Electrochem.* **31** (1995) 1299.

17. S. Fletcher, C.S. Halliday, D. Gates, M. Westcott, T. Lwin, G. Nelson, *J. Electroanal. Chem.* **159** (1983) 267.

18. A. Milchev and M.I. Montenegro, *J. Electroanal. Chem.* **333** (1992) 93.

19. Southampton Electrochemical Group, *Instrumental Methods in Electrochemistry*, Ellis Horwood, Chichester, 1990, Chapter 9.

20. V.D. Jovic, N. Tosic and M. Stojonovic, *J. Electroanal. Chem.* **430** (1997) 43.

21. V.D. Jovic, R.M. Zejnilovic, A.R. Despic and J.S. Stevanovic, *J. Appl. Electrochem.* **18** (1988) 511.

22. E. Vallés, R. Pollina and E. Gómez, *J. Appl. Electrochem.* **23** (1993) 508.

23. E. Gómez, M. Marin, F. Sanz and E. Vallés, *J. Electroanal. Chem.* **422** (1997) 139.